

MAXIMUM POWER POINT TRACKING FOR PV SYSTEMS USING ARTIFICIAL NEURAL NETWORKS

TIAGO TARGINO SEPULVEDA*, LUCIANA MARTINEZ*, ANDRÉ PIRES NÓBREGA TAHIM*

**Rua Professor Aristides Novis, nº 02, Federação, CEP 40210-630
Departamento de Engenharia Elétrica, UFBA
Salvador, Bahia, Brasil*

Emails: tiago.targino@ufba.br, lucianam@ufba.br, atahim@ufba.br

Abstract— This paper proposes a method of maximum power point tracking for photovoltaic (PV) panels using neural networks. The PV system consists of a solar panel, a DC-DC converter, a control system and the load. Two neural networks will be trained to integrate into the system. The first network is responsible for estimating the level of solar irradiance from the electric current, voltage and temperature signals of the solar panel. The second neural network is connected to the first and uses its output (irradiance) with the temperature to generate a reference voltage, corresponding to the maximum power voltage, to a PI controller. The system's response under variable conditions of irradiance, temperature and load will be analyzed, as well as a performance comparison with the incremental conductance method. Results show that the artificial neural network was able to detect the maximum power point under dynamics behavior quicker than the incremental conductance, hence, maximizing the power transferred to the load.

Keywords— Photovoltaic system, Maximum power point tracking, Artificial Neural Network

Resumo— Este trabalho propõe um método de rastreamento do ponto de máxima potência para painéis fotovoltaicos (PV) utilizando redes neurais. O sistema PV consiste em um painel solar, um conversor DC-DC, um sistema de controle e a carga. Duas redes neurais serão treinadas para integrar ao sistema. A primeira rede é responsável por estimar o nível de irradiação solar a partir dos sinais de corrente, tensão e temperatura do painel solar. Já a segunda rede neural é conectada a primeira e utiliza sua saída (irradiação) junto com a temperatura para gerar uma tensão de referência, respectiva a tensão de máxima potência, a um controlador PI. Serão analisados as respostas do sistema sob condições variáveis de irradiação, temperatura e carga, além de um comparação de performance com o método da condutância incremental. Os resultados apresentados mostram que a rede neural artificial foi capaz de detectar o ponto de máxima potência sob condições dinâmicas mais rápido do que o método da condutância incremental, portanto, maximizando a potência transferida para a carga.

Palavras-chave— Sistemas fotovoltaicos, Rastreamento do ponto de máxima potência, Redes neurais artificiais

1 Introduction

The use of solar energy for electric power generation has become increasingly common, not only because it is a type of renewable energy but mainly because it is a source of clean, inexhaustible, free and widely available energy.

To perform the conversion of light into electricity, photovoltaic (PV) modules, composed of semiconductor material, were developed using the principle of the photovoltaic effect. Among the semiconductors materials, most of the panels available on the market are composed of monocrystalline silicon and polycrystalline silicon for being more efficient and reliable (Pinho, 2014).

However, the power supplied through these panels may not be the maximum available. The reason is the dependence of different factors that influence the power generation and operation point of the photovoltaic panels, such as: connected load, cell temperature and incident irradiance value. Because of this, usually, a DC-DC converter is connected to the output of the panel in order to guarantee the generation of maximum available power, regardless of the factors mentioned previously.

The main point for optimizing the system is

to control the duty cycle (D) through a control based on the principle of Maximum Power Tracking (MPPT). Among the most known methods are the Constant Voltage (CV), which is made to ensure that the panel operates at the voltage respective to the Maximum Power Point (MPP). The Perturb and Observe method (P&O) is based on the variation of the output voltage of the PV module and calculate the power obtained from this variation. The Incremental Conductance method (InC) uses the value of the derivative of the power by the voltage to determine the direction of the MPP (Salas et al., 2006).

However, these MPPT methods have its own advantages and drawbacks. Besides the easy implementation, the CV method is not very effective to temperature's influence because the voltage at MPP is very sensible to temperature. The P&O method has the disadvantages of poor efficiency at low irradiance, oscillations around MPP and rapid changes of irradiation may lead the tracking to a wrong direction of MPP causing energy loss in the process (Babaa et al., 2014). The InC method generally presents better results than the others, but, it has a drawback of possible instability due the calculation of derivatives. Also, these calculations may require big computational effort and

under low levels of irradiance, the differentiation results become deficient (Liu et al., 2004).

Other tracking models use training-based methods such as neural networks, fuzzy logic and genetic algorithms, which are used to obtain a rapid system response to locate the maximum power point. In the case of neural networks, the procedure is usually done by performing a training which input parameters are the values of irradiance and temperature submitted to the solar panel and the output is voltage respective to the maximum power point. This voltage is used as reference in a system formed by a controller and a Pulse Width Modulation (PWM) circuit, thus generating the respective duty cycle value for the DC-DC converter (Salah and Ouali, 2011), (Martin and Vazquez, 2015) and (Dkhichi et al., 2016).

This paper aims to use an Artificial Neural Network (ANN) to determine the maximum power point in a solar panel using Matlab/Simulink software. For this, two different networks will be trained and then interconnected. The first one will be responsible for estimating the level of local solar irradiance from the temperature, electric current and voltage signals. The second one will use the irradiation level (estimated by the previous neural network) and the temperature signal to generate reference voltage. The results will analyze the effectiveness in tracking for different levels of irradiance, temperature and load.

This work is organized as follows: The description and models of the solar panel and DC-DC converter considered in the system are discussed in section 2. Section 3 presents the details of the neural networks implemented. The results and discussions are presented in section 3 and then the conclusions in section 4.

2 System descriptions

The system to be implemented is illustrated in Figure 1. It is composed by the generation in the PV panel, the ANN, a power stage composed by the DC-DC converter, the control and the load connected through the DC-DC converter. The control is performed by a PI controller which receives the error between the reference voltage and the variable measured. The proportional value (P) uses the error value to produces a proportional output while the integral value (I) uses the cumulative error to accelerate the output to reach the reference.

2.1 Modeling of Solar Panel

Figure 2 shows the electric model of a solar cell proposed by (Gow and Manning, 1999). This is the model commonly adopted in works that involve the simulation of a solar panel, because, in

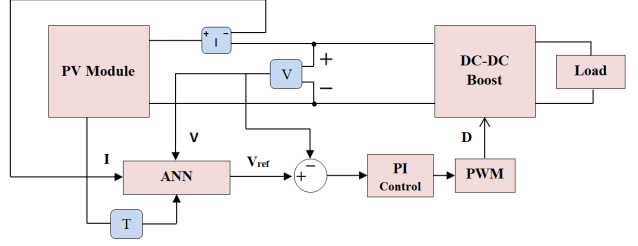


Figure 1: Schematic for the complete system.

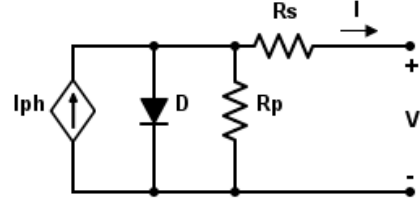


Figure 2: Equivalent circuit of a photovoltaic cell.

addition to being simple, the model incorporates the intrinsic losses of a solar cell which are essential to the simulations become closer to the real values. The current source I_{ph} represents the electric current generated from the solar irradiance (G), V , the voltage at the output terminals, R_s e R_p the series and parallel resistors respectively. The electric current I provided by the solar cell can be expressed by equation (1).

$$I = I_{ph} - I_o \cdot \left[e^{\frac{q \cdot (V + I \cdot R_s)}{n \cdot K \cdot T}} - 1 \right] - \frac{V + I \cdot R_s}{R_p} \quad (1)$$

where I_o is the reverse saturation current of the cell, q is the charge of the electron, n is the ideality factor, K is the Boltzmann constant, and T is the cell temperature. The electric current I_{ph} can be calculated by (2) which depends on the incident radiation G :

$$I_{ph} = [I_{sc} + \alpha_t \cdot (T - T_r)] \cdot \frac{G}{1000} \quad (2)$$

where I_{sc} is the short-circuit current of the cell, α_t is the temperature coefficient of the short-circuit current and T_r is the reference temperature. Finally, the reverse saturation current I_o is dependent of the cell temperature and can be calculated by:

$$I_o = I_{o_{ref}} \cdot \left(\frac{T}{T_r} \right)^3 \cdot e^{\left[\frac{q \cdot E_G}{n \cdot k} \cdot \left(\frac{1}{T_r} - \frac{1}{T} \right) \right]} \quad (3)$$

Electrical specifications considered in this paper were obtained from a commercial low-power solar panel (Supply, 2018). The solar module chosen for simulations is a monocrystalline type ca-

pable of generating 20W under standard test conditions (STC). Table 1 shows the characteristics of the photovoltaic module under the STC.

From the presented equations and the informations of Table 1 it is possible to generate as characteristic curves of a solar panel varying voltage and temperature and obtaining the value of the respective electric current. Figure 3 shows the influence of irradiance on current-voltage (IV) and power-voltage (PV) curves while keeping the temperature constant at 25°C. On the other hand, Figure 4 shows the temperature's influence on IV and PV curves when the irradiance is constant at 1000W/m².

Table 1: Electrical characteristics of 420J-20W Photovoltaic module under Standard Test Conditions (STC)

Electrical characteristics	STC
Maximum power (P_{max})	20W
Voltage at Pmax (V_{mp})	16.8V
Current at Pmax (I_{mp})	1.19A
Open circuit voltage (V_{oc})	21.0V
Short circuit current (I_{sc})	1.29A
Temperature coefficient de I_{sc}	0.105%/°C

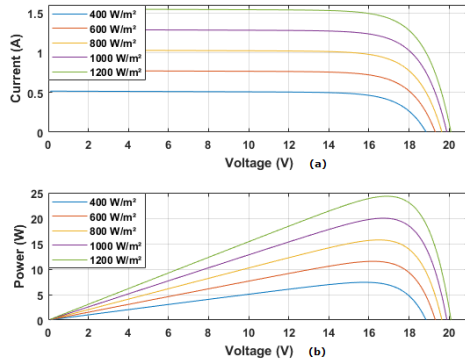


Figure 3: IV (a) and PV (b) curves at various levels of irradiance when T=25°C.

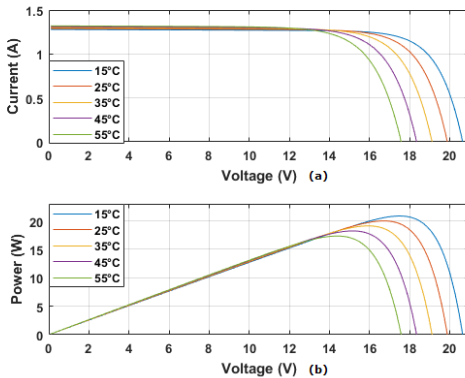


Figure 4: IV (a) and PV (b) curves at various levels of temperature when G= 1000W/m².

2.2 Boost Converter

It is known that the power provided by the photovoltaic panels depends on the weather conditions and the load that are interconnected. One way to ensure that the panel operates at the maximum available power is to connect a DC-DC converter to lead the operating point of the PV panel to the maximum power point.

The configuration of the boost converter is shown in Figure 5. Considering that the converter must operate in the continuous conduction mode, the capacitance (C) and inductance (L) values used were 2μF and 10mH.

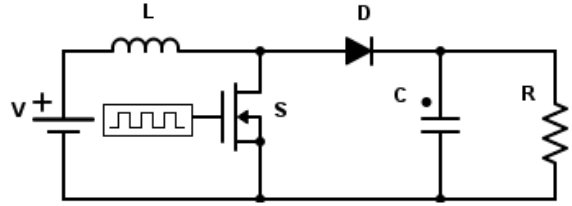


Figure 5: DC-DC boost converter.

The control in the converter is performed through Pulse Width Modulation (PWM) and switching devices such as IGBT or MOSFET. The output of the PI control block is the modulator to be compared to the 20 kHz triangular carrier, thus generating Pulse Width Modulation (PWM) which commands the opening / closing of the Boost switch as seen in Figure 6. Therefore, it is through the duty cycle D of the Boost converter that the operating point of the modules for the Maximum Power Point is shifted.

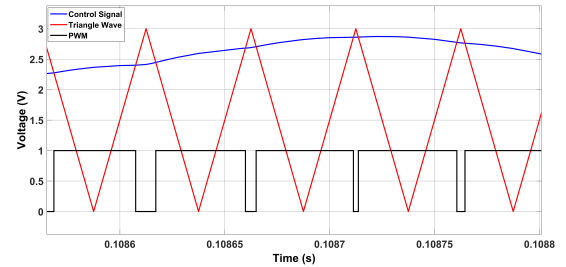


Figure 6: PWM signal generation with a triangular reference.

3 Artificial Neural Networks

The artificial neural networks were build and trained using the neural network toolbox from Matlab (Figure 7). The neural network proposed in the work will be divided into two parts: The first one will be responsible for estimating the level of solar irradiance (G) from the voltage (V), electric current (I) and temperature (T) measurements of the photovoltaic panel. With the values

of irradiance and temperature it will be possible to determine a reference voltage from a second neural network connected with the first one, as shown in Figure 8. Thus, the proposed system will replace a solar irradiance sensor, potentially costly equipment to a project of smaller proportions, by current and voltage sensors, which are feasible for any project.

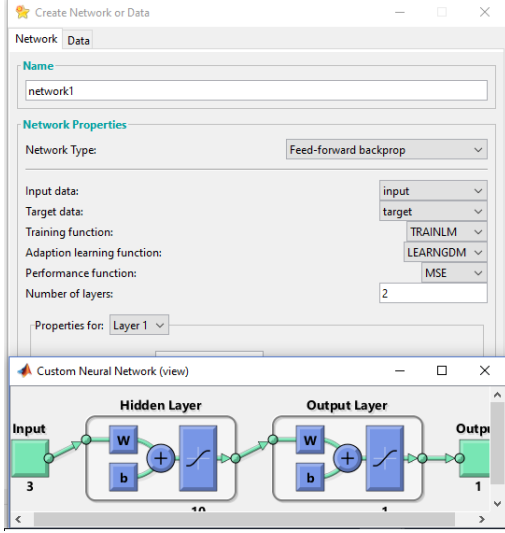


Figure 7: Matlab neural network toolbox overview

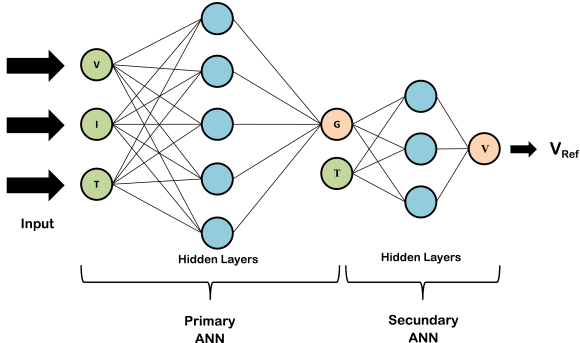


Figure 8: Schematic diagram of the artificial neural network proposed.

3.1 Training

The neural network training was performed using back-propagation's method adopting the Levenberg-Marquardt algorithm. For the first neural network training, 18216 samples of temperature, electrical current and voltage signals were used to estimate irradiance values between 100 and 1200 W/m^2 . The result of training is shown in Figure 9.

The second neural network training was performed using 96 samples of temperature (from 15° to 50°C with a step of 5°C) and irradiance (from 100 W/m^2 to 1100 W/m^2 with a step of

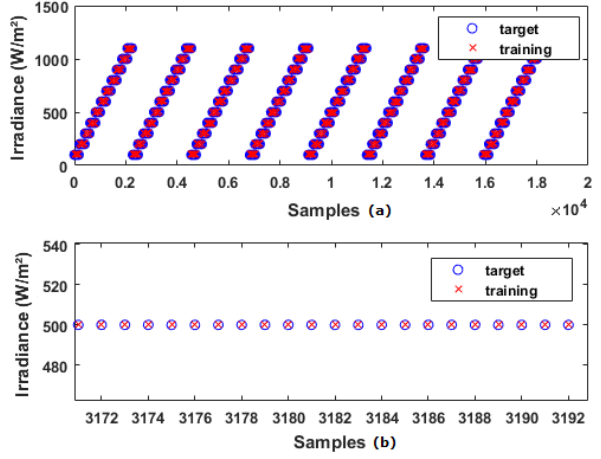


Figure 9: Result of first neural network training (a); Close up view of results (b).

100 W/m^2) to estimate the reference voltage. Result is shown in Figure 10.

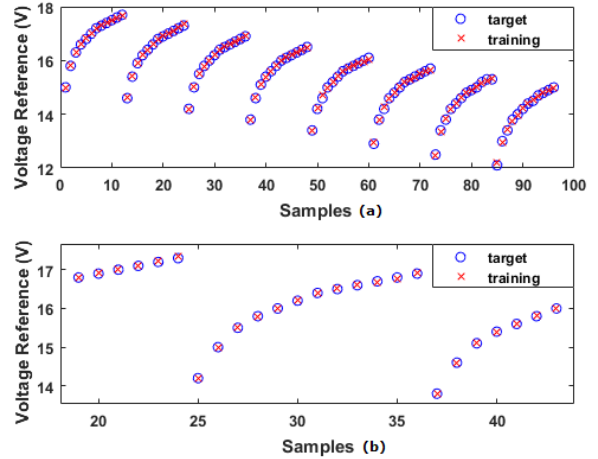


Figure 10: Result of second neural network training (a); Close up view of results (b).

In order to verify the effectiveness of the training, three prediction error measures were calculated: The Average Percentage Absolute Error (APAE); Mean Bias Error (MBE) and Root Mean Square Error (RMSE). The equations are given below, where m is the total number of samples; y_i is i^{th} real value of sample; e_i is the i^{th} estimated value by the neural network (Essefi et al., 2014).

$$APAE = \frac{1}{m} \sum \left(\frac{|y_i - e_i|}{y_i} \right) \quad (4)$$

$$MBE = \frac{1}{m} \sum \left(\frac{e_i - y_i}{y_i} \right) \quad (5)$$

$$RMSE = \sqrt{\frac{1}{m} \sum \left(\frac{e_i - y_i}{y_i} \right)^2} \quad (6)$$

4 Results and discussions

Next, the results will be presented when the trained artificial neural network (Figure 8) is inserted in the PV system.

Table 2 shows the prediction errors for the ANN. Results show small errors for the three parameters, therefore, the neural network is able to estimate values with good precision. However, it is seen that the RMSE penalizes large errors more than the others.

Table 2: Prediction errors for the trained ANN

Error	Value
Average Percentage Absolute Error	0.0005%
Mean Bias Error	0.0009%
Root Mean Square Error	0.0096%

Table 3 and 4 bring general results when varying irradiance and temperature levels respectively but keeping the load constant at $1k\Omega$. Where P_{ref} is the maximum power reference (obtained from the model developed previously), P is the measured power output of the PV panel from the simulink simulations and η_{pv} is the efficiency given by $\frac{P}{P_{ref}} \cdot 100\%$

Table 3: Tracking efficiency of Neural Network's method ($T=25^\circ C$).

$G(W/m^2)$	$P_{ref}(W)$	$P(W)$	η_{pv}
300	5.403	5.402	99.99%
350	6.404	6.403	99.99%
400	7.415	7.413	99.98%
450	8.434	8.431	99.96%
500	9.461	9.456	99.95%
550	10.494	10.492	99.98%
600	11.533	11.530	99.98%
650	12.577	12.572	99.96%
700	13.625	13.619	99.96%
750	14.679	14.667	99.92%
800	15.736	15.723	99.91%
850	16.797	16.780	99.90%
900	17.862	17.840	99.87%
950	18.930	18.925	99.97%
1000	20.002	19.995	99.97%
1050	21.075	21.060	99.93%
1100	22.153	22.133	99.91%

Table 4: Tracking efficiency of Neural Network's method ($G=1000 W/m^2$).

$T(^{\circ}C)$	$P_{ref}(W)$	$P(W)$	η_{pv}
15	20.863	20.851	99.94%
20	20.434	20.428	99.97%
25	20.002	19.998	99.98%
30	19.570	19.561	99.95%
35	19.135	19.123	99.93%
40	18.794	18.680	99.39%
45	18.243	18.228	99.91%
50	17.797	17.774	99.87%
55	17.347	17.329	99.89%

Results show an effectiveness above 99% in tracking the maximum power point considering different levels of irradiance and temperature.

Figure 11 shows how the neural network performs in tracking the MPP compared to Incremental Conductance's method (InC) when applied two different values of irradiance (1000 and $400 W/m^2$). It is possible to see that the ANN method reaches the reference value quicker (0.025s) and with lower overshoot while the incremental conductance takes almost 0.3s to stabilize in the reference. The same occurs when the irradiance is modified to $400 W/m^2$. Similarly, Figure 12 compares the two methods when submitted to different temperatures keeping the irradiance constant. In the same way, the ANN reaches the reference more quickly when compared to InC.

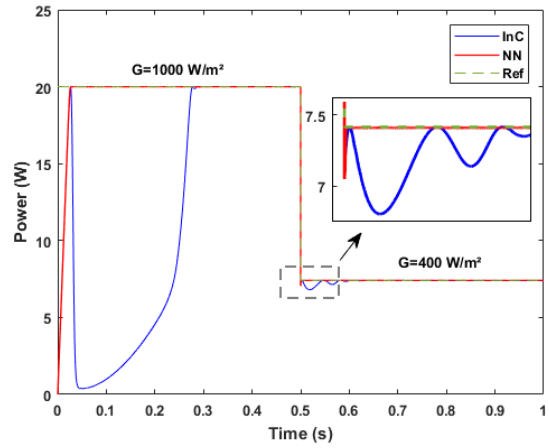


Figure 11: Comparative of InC (blue) and ANN (red) methods for $R=1k\Omega$, $T=25^\circ C$.

Figure 13 presents the performance of the system when the load is variable ($1M\Omega$, $10k\Omega$ and 100Ω) and considering irradiance and temperature constant. Because it was chosen to use the boost topology as a dc-dc converter it is expected that lower values of load would produce more instability in the system. However, for values above 100Ω it is shown that the variance of response is minimum. Without an appropriate control, this change of load would shift the operation point and

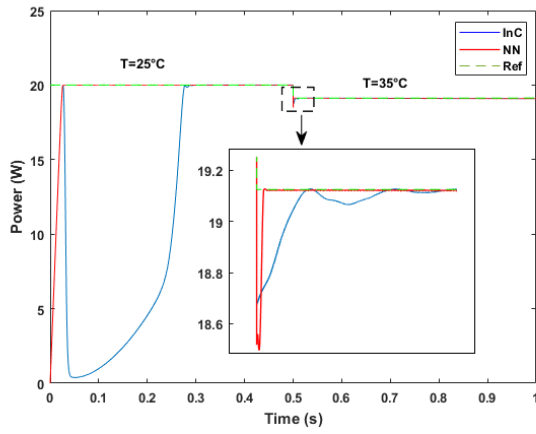


Figure 12: Comparative of InC (blue) and ANN (red) methods for $R=1k\Omega$, $G = 1000W/m^2$.

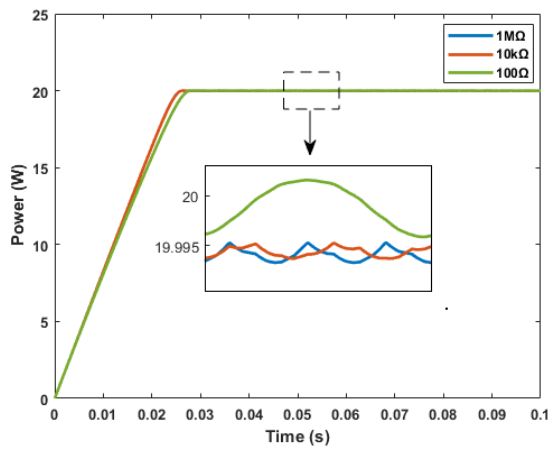


Figure 13: Performance of ANN's method for different loads $T=25^\circ C$, $G = 1000W/m^2$.

therefore the maximum power point would not be achieved. The ability of the system to deliver maximum power even with a high load variation reveals the effectiveness of the applied control.

5 Conclusions

In this paper it was developed an artificial neural network applied to PV maximum power point tracking composed by two stages. The first was designed to estimate irradiance based on values of electric current, voltage and temperature. While the second stage uses the irradiance estimated and temperature to obtain the reference voltage. It was shown that based on a training data, the neural network achieved better results than a incremental conductance's method, specially under environmental changes of irradiance and temperature when the transitory time was significantly decreased when the ANN was applied compared to the INC method. Furthermore, the system also performed with good accuracy when

submitted to a load variance, being able to track the maximum power point even though large variance of load.

References

- Babaa, S. E., Armstrong, M. and Pickert, V. (2014). Overview of maximum power point tracking control methods for pv systems, *Journal of Power and Energy Engineering* **2**(08): 59.
- Dkhichi, F., Oukarfi, B., Ouoba, D., Fakkar, A. and Achalhi, A. (2016). Behavior of neural network mppt technique on a pv system operating under variable load and irradiation, *Electrical Sciences and Technologies in Maghreb (CISTEM), 2016 International Conference on*, IEEE, pp. 1–4.
- Essefi, R. M., Souissi, M. and Abdallah, H. H. (2014). Maximum power point tracking control using neural networks for stand-alone photovoltaic systems, *International Journal of Modern Nonlinear Theory and Application* **3**(03): 53.
- Gow, J. and Manning, C. (1999). Development of a photovoltaic array model for use in power-electronics simulation studies, *IEE Proceedings-Electric Power Applications* **146**(2): 193–200.
- Liu, C., Wu, B. and Cheung, R. (2004). Advanced algorithm for mppt control of photovoltaic systems, *Canadian Solar Buildings Conference, Montreal*, Citeseer, pp. 20–24.
- Martin, A. D. and Vazquez, J. R. (2015). Mppt algorithms comparison in pv systems: P&co, pi, neuro-fuzzy and backstepping controls, *Industrial Technology (ICIT), 2015 IEEE International Conference on*, IEEE, pp. 2841–2847.
- Pinho, João Tavares e Galdino, M. A. (2014). Manual de engenharia para sistemas fotovoltaicos, *Rio de Janeiro* pp. 47–63.
- Salah, C. B. and Ouali, M. (2011). Comparison of fuzzy logic and neural network in maximum power point tracker for pv systems, *Electric Power Systems Research* **81**(1): 43–50.
- Salas, V., Olias, E., Barrado, A. and Lazaro, A. (2006). Review of the maximum power point tracking algorithms for stand-alone photovoltaic systems, *Solar energy materials and solar cells* **90**(11): 1555–1578.
- Supply, S. E. (2018). Ses-420j data sheet. [<https://www.solarelectricsupply.com/solar-electric-supply-ses-420j-solar-panels-540>, Acesso 9-Fevereiro-2018].